Paper submitted to
Inter-noise 2022
21-24 August 2022
Scottish Event Campus
Glasgow

The influence of model assumptions in a hybrid prediction tool for railway induced vibration

David Thompson[1], Evangelos Ntotsios
ISVR, University of Southampton
Highfield, Southampton SO17 1BJ, UK

Pascal Bouvet, Brice Nélain, Sylvain Barcet
Vibratec
28 Chemin du petit bois, F-69131, Ecully, France

Andreas Nuber, Bernd Fröhling
Wölfel Engineering GmbH + Co. KG
Max-Planck Strasse 15, D-97204 Höchberg, Germany

Pieter Reumers, Fakhraddin Seyfaddini, Geertrui Herremans, Geert Lombaert, Geert Degrande
KU Leuven, Department of Civil Engineering
Kasteelpark Arenberg 40, B-3001 Leuven, Belgium

ABSTRACT

Within the SILVARSTAR project, a user-friendly frequency-based hybrid prediction tool is developed to assess the environmental impact of railway induced vibration. This will be implemented in the existing noise mapping software IMMI. The vibration level in a building in each frequency band is expressed as the product of source, propagation and receiver terms. A hybrid approach is used that combines experimental data with numerical predictions, providing increased flexibility and applicability. The train and track properties can be selected from a database or as numerical values. The user can select soil impedance and transfer functions from a database, pre-computed for a wide range of parameters with the MOTIV and TRAFFIC models. An experimental database of force densities, transfer functions, free field vibration and input parameters is also integrated into the new tool. The building response is estimated by means of empirical correction factors. Assumptions within the modelling approach can influence the prediction accuracy and the present paper aims to quantify these. We focus on the influence of train speed and soil properties on the compliance of the track-soil system and the free field response.

1. INTRODUCTION

In recent years a variety of different modelling approaches have been developed for train-induced vibration that can be used to assess the environmental impact of new railway lines or the extension of existing lines [1]. However, many models are computationally expensive and there is a lack of uniformity, which makes it difficult to compare results obtained with different models. Moreover, the quality of the predictions and the associated uncertainty strongly depend on the available data and the

[1] djt@isvr.soton.ac.uk

experience of the users. Existing models are not well integrated in the railway project development process and there is a general lack of user-friendly software incorporating widely accepted solution methods. A major objective of the SILVARSTAR project [2,3] is therefore to develop a user-friendly efficient prediction tool to assess the environmental impact of railway induced vibration at a system level. This is being implemented in the existing noise mapping software IMMI.

To ensure that the modelling approach is sufficiently efficient, various simplifying assumptions must be introduced. However, the prediction accuracy is influenced by these assumptions. In particular, the train speed and soil properties influence the compliance of the track-soil system, the dynamic axle loads, and the free field response. Following a brief introduction to the frequency-based hybrid modelling approach adopted, these modelling assumptions are discussed.

2. OVERVIEW OF THE MODELLING APPROACH

2.1. General Framework

The proposed SILVARSTAR modelling approach is based on the assumption that the vibration in each one-third octave frequency band can be expressed as the product of source, propagation and receiver terms [4,5]. The vibration level in a building $A(f)$ at frequency f is written as the product of a source term $S(f)$ for the vehicle-track interaction, a propagation term $P(f)$ for the soil and a receiver term $R(f)$ for the building:

$$A(f) = S(f)\, P(f)\, R(f) \tag{1}$$

or equivalently as a sum of terms in decibels. Each of these frequency-dependent terms can be represented by numerical predictions or by experimental data. One advantage is that a hybrid approach is possible combining experimental data with numerical predictions, providing increased flexibility and applicability. This equation omits Doppler effects due to moving sources. However, it is expected to provide reasonable results when the train speed is relatively low compared with the wave velocities in the soil, while maintaining low calculation times.

2.2. Fully empirical prediction scheme

The empirical procedure adopted is based on FTA guidelines [4]. The vibration velocity level $\mathrm{L_v}(\mathbf{x}_\mathrm{b})$ at a receiver $\mathbf{x}_\mathrm{b}$ in the building (see Figure 1a) is expressed in decibels in one-third octave bands as a sum of source, propagation, and receiver terms:

$$\mathrm{L_v}(\mathbf{x}_\mathrm{b}) = \mathrm{L_F}(\mathbf{X}, \mathbf{x}_1) + \mathrm{TM_L}(\mathbf{X}, \mathbf{x}_1) + \mathrm{C_b}(\mathbf{x}_1, \mathbf{x}_\mathrm{b}) \tag{2}$$

where $\mathrm{L_F}(\mathbf{X}, \mathbf{x}_1)$ is the equivalent force density level, $\mathrm{TM_L}(\mathbf{X}, \mathbf{x}_1)$ is the line source transfer mobility and $\mathrm{C_b}(\mathbf{x}_1, \mathbf{x}_\mathrm{b})$ is the building's coupling loss, which is computed as a combination of adjustment factors from the RIVAS project [6] or could be obtained directly from measurement.

(a) (b)

Figure 1: (a) Source, soil and receiver positions; (b) excitation and receiver locations for line source transfer mobility measurements.

The line source transfer mobility can be derived from the superposition of point source transfer mobilities $\mathrm{TM_P}(\mathbf{X}_k, \mathbf{x}_1)$ for a series of n equidistant source points $\mathbf{X}_k$ with spacing h (see Figure 1b):

$$\mathrm{TM_L}(\mathbf{X}, \mathbf{x}_1) \;=\; 10\log_{10}\left[\; h \sum_{k=1}^{n} \; 10^{\frac{\mathrm{TM_P}(\mathbf{X}_k, \mathbf{x}_1)}{10}}\right] \tag{3}$$

The force densities can be obtained from the measured vibration level during train pass-by and line source transfer mobility by rearranging Equation 2 (omitting the building's coupling loss term):

$$\mathrm{L_F}(\mathbf{X}, \mathbf{x}_1) = \mathrm{L_v}(\mathbf{x}_1) - \mathrm{TM_L}(\mathbf{X}, \mathbf{x}_1) \tag{4}$$

2.3. Fully numerical prediction scheme using a modular approach

An analytical train-track interaction model is integrated in the prediction tool and used to compute the wheel-rail contact forces and the forces transmitted to the ground. The vehicle is represented by a simple multi-body model (Figure 2a). The track (Figure 2b) may be ballasted or slab and is modelled by Euler-Bernoulli beams for the rail (and slab) with resilient layers for rail pads, under-sleeper pads, ballast, and slab mat.

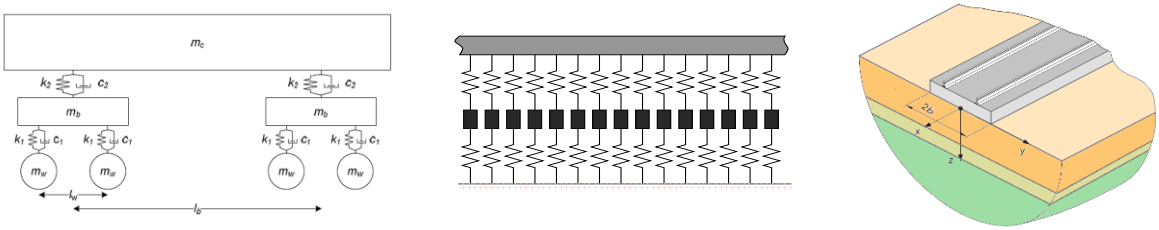

(a) (b) (c)

Figure 2: (a) Vehicle model; (b) ballasted track model; (c) example of track on layered soil.

The track is coupled to the ground over a finite width (Figure 2c). The ground is represented by impedances in the frequency-wavenumber domain that are pre-computed for a range of soil parameters using the MOTIV [7] and TRAFFIC models [8]. These cover homogeneous and layered soils. The train-track interaction problem is solved in the frequency domain, considering the excitation due to rail and wheel unevenness. The force transmitted to the subgrade is then estimated in the wavenumber domain and the free field ground response is calculated using pre-computed soil transfer functions, obtained using the same models. The response due to a train passage is obtained by summation of the contribution of each axle. The transfer to the building is treated in the same way as in the empirical prediction scheme.

2.4. Hybrid prediction schemes

Hybrid prediction schemes are also included in which numerical and empirical data are combined, following Equation 2, providing more flexibility than purely experimental or numerical models. Two options are available: a numerical source model combined with an empirical propagation term and an empirical source model combined with a numerical propagation term. More details on hybrid approaches can be found in references [9,10].

3. THE INFLUENCE OF MODELLING ASSUMPTIONS

The frequency-based approach used in the vibration prediction tool relies on various modelling assumptions. This section compares the effect on the results of these different approximations for a range of practical parameters and highlights the differences in the free field response calculated by considering each approach. These calculations are made using the TRAFFIC model [8] and have been benchmarked against results from MOTIV [7].

3.1. Parameters

A typical ballasted track is considered for which the rails are modelled as Euler-Bernoulli beams and the railpads are considered as continuous springs between the rails and the sleepers. The sleepers are assumed to be rigid masses and the ballast bed is assumed to act as a layer of linear springs and dampers. The track properties are summarised in Table 1.

Table 1: Track properties for ballasted track.

Rail	Bending stiffness per rail ($MN \cdot m^2$)	6.42
	Mass per unit length per rail (kg/m)	60
Rail pad	Stiffness per pad (MN/m)	150
	Damping loss factor	0.3
	Fastener spacing (m)	0.6
Sleeper	Mass (kg)	325
	Length (m)	2.6
Ballast	Mass per unit length (kg/m)	1485
	Stiffness per unit length (MN/m^2)	830
	Damping loss factor	0.15
	Lower width (m)	3.6

A nominal Intercity (IC) train is considered in this study consisting of four identical vehicles. Each vehicle is a 10-DOF model consisting of the vehicle body, two bogies, four axles, as well as primary and secondary suspensions. The properties of the train are given in Table 2. The track unevenness is based on track quality class 6 from the Federal Railroad Administration (FRA) guidelines.

Table 2: Vehicle properties of the IC train.

Car body	Mass (kg)	40000
	Pitching moment of inertia ($kg \cdot m^2$)	$2 \cdot 10^6$
	Vehicle length (m)	23
Bogie	Mass (kg)	5000
	Pitching moment of inertia ($kg \cdot m^2$)	6000
	Bogie distance (m)	17
Wheelset	Mass (kg)	1200
	Wheelset distance (m)	2.5
	Contact stiffness (per wheel, GN/m)	1.26
	Total axle load (kN)	114.8
Primary suspension	Vertical stiffness per axle (MN/m)	2.0
	Vertical viscous damping per axle ($kN \cdot s/m$)	40
Secondary suspension	Vertical stiffness per bogie (MN/m)	0.5
	Vertical viscous damping per bogie ($kN \cdot s/m$)	31.6

Three homogeneous grounds are considered, characterised as soft, medium, and stiff soil. The dynamic soil characteristics are summarised in Table 3, in terms of the shear (S-) wave speed, dilatational (P-) wave speed, density, and isotropic material damping ratio.

Table 3: Ground properties.

Parameters of soil	**Soft**	**Medium**	**Stiff**
S-wave speed (m/s)	100	200	400
P-wave speed (m/s)	200	400	800
Density (kg/m^3)	1800	1800	1800
Damping ratio	0.025	0.025	0.025

3.2. Free field response

The vibration spectrum is calculated for the full passage of the IC train at three train speeds: 50 km/h, 150 km/h and 300 km/h. The vertical vibration velocity levels L_v at the ground surface due to the passage of the train are shown in Figures 3 and 4 for two different distances from the track, 8 m and 32 m. The response is shown as the average one-third octave band spectrum which includes only the contribution of the dynamic excitation (due to the rail unevenness) and ignores the quasi-static excitation (due to the moving axle loads). For higher speeds the vibration level increases and the frequency content is more concentrated at higher frequencies, whereas for softer soil the vibration is stronger at low-mid frequencies and attenuated by damping at high frequencies.

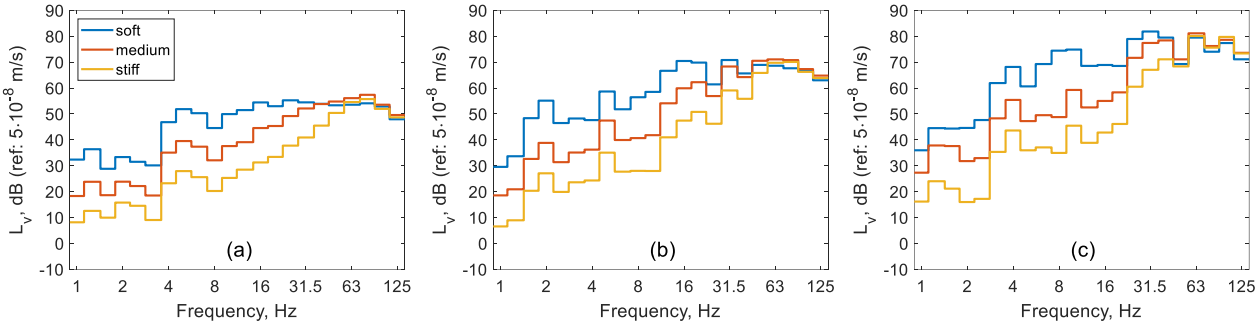

Figure 3: Free field vibration level L_v at 8 m from the track for the IC train running with (a) 50 km/h, (b) 150 km/h and (c) 300 km/h.

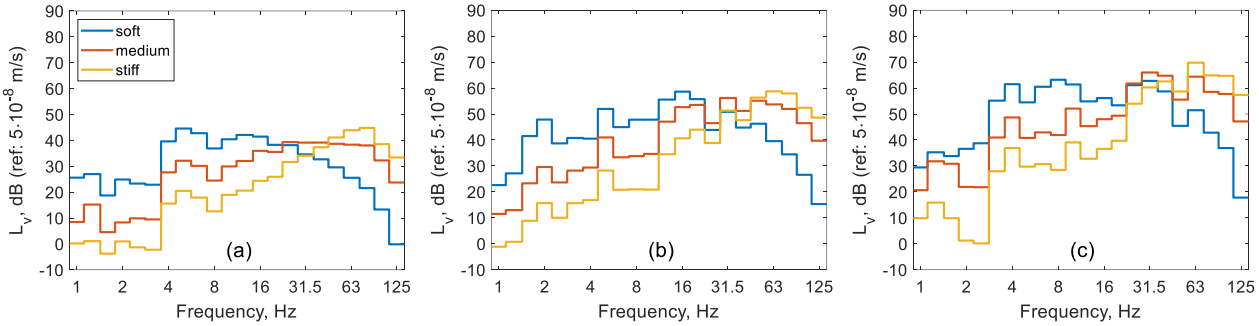

Figure 4: Free field vibration level L_v at 32 m from the track for the IC train running with (a) 50 km/h, (b) 150 km/h and (c) 300 km/h.

In the following, results will be presented as the vibration level difference ΔL_v in dB between the response calculated by assuming a modelling approximation $L_{v,approx}$ and the response calculated for a reference case $L_{v,ref}$ that does not consider the specific approximation in the modelling approach:

$$\Delta L_v = L_{v,approx} - L_{v,ref} \tag{5}$$

3.3. Effect of speed on track compliance

The track compliance has been calculated for the three soil conditions considering a stationary load and a load moving at the highest speed of 300 km/h. The magnitude of the track compliance is shown in Figure 5. There are some differences for the soft soil below about 30 Hz but at higher frequencies, and for the other two soil types, the track compliances show good agreement.

The vibration level difference ΔL_v between the free field response calculated using the track compliance due to the non-moving loads and that for the 300 km/h moving loads are shown in Figure 6 for the soft soil. Even though this is the most extreme case, the level difference is less than 1 dB, meaning that the influence of the moving load on the track compliance does not affect the vibration predictions in the free field.

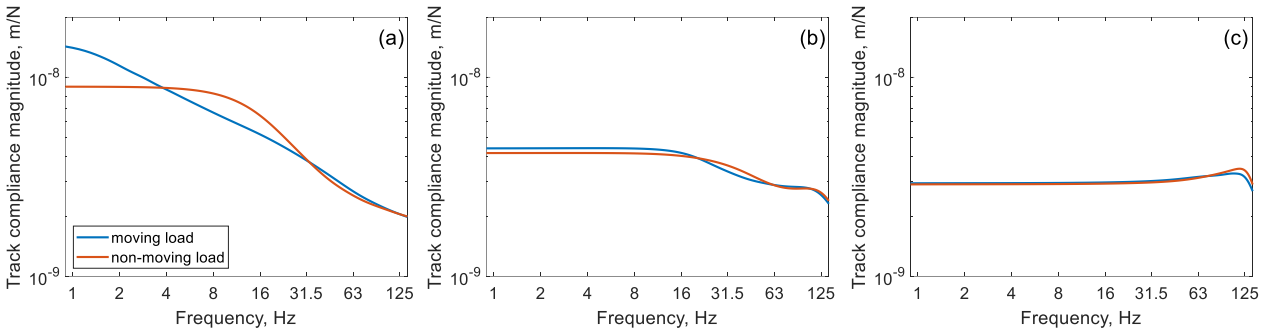

Figure 5: Track compliance magnitude for the (a) soft soil, (b) medium soil and (c) stiff soil for the IC train running at 300 km/h.

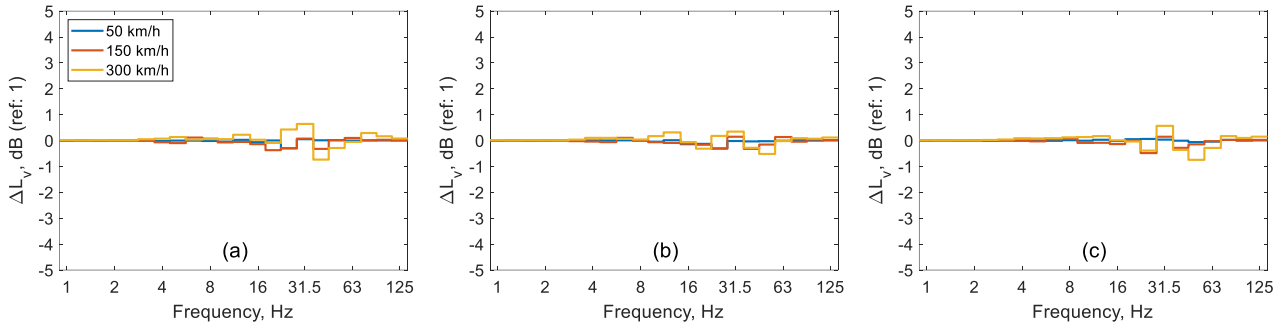

Figure 6: Free field vibration level difference ΔL_v between the non-moving load approximation and the moving load reference for the calculation of the track compliance at (a) 8 m, (b) 16 m and (c) 32 m from the track for the IC train running with different speeds at the soft soil site.

3.4. Low-speed approximation

The free field vibration amplitude increases when the train approaches, is almost stationary during the train passage, and decreases once the train has passed. The low-speed approximation aims to predict the stationary part of the response by assuming fixed axle positions. As a result, the Doppler shift between the frequency content of the receiver and the source is disregarded. Figures 7 and 8 show the vibration level difference ΔL_v between the response calculated with the low-speed approximation and the moving train response for the three trains speeds. Overall, the differences increase when the train speed increases and are more than 10 dB in individual frequency bands at the highest speed. Nevertheless, these differences mainly correspond to a redistribution of energy into different bands due to the Doppler effect and the overall vibration level summed over all frequency bands is affected much less, with differences of 2-3 dB.

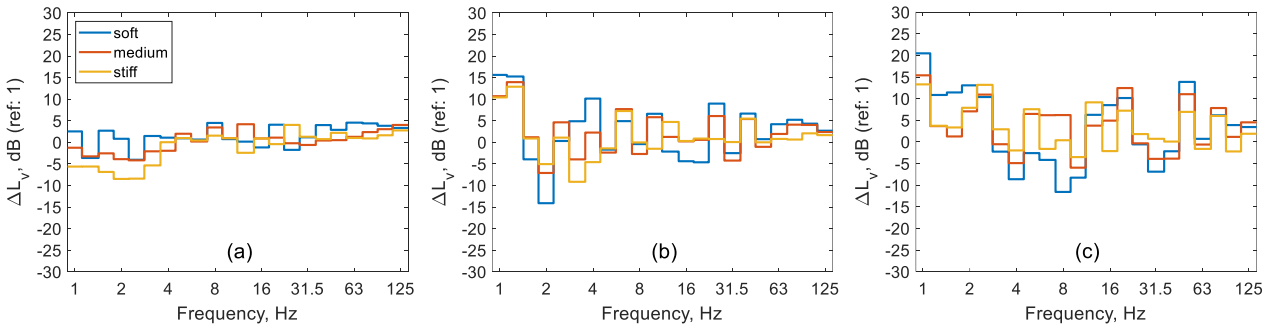

Figure 7: Free field vibration level difference ΔL_v between the low-speed approximation and the moving train response at 8 m from the track for the IC train running with (a) 50 km/h, (b) 150 km/h and (c) 300 km/h.

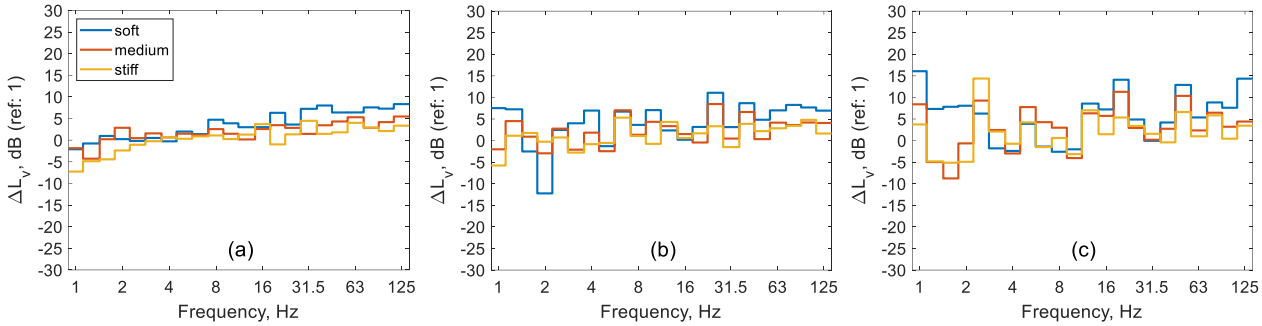

Figure 8: Free field vibration level difference ΔL_v between the low-speed approximation and the moving train response at 32 m from the track for the IC train running with (a) 50 km/h, (b) 150 km/h and (c) 300 km/h.

3.5. Independent dynamic axle loads

In the vibration prediction tool, the free field response is calculated using non-moving dynamic axle loads that are assumed to be incoherent, whereas in the full model they are assumed to be excited by the same unevenness apart from a time lag. The vibration level difference between results based on this approximation and the reference case (in this case for non-moving but coherent axle loads) is shown in Figures 9 and 10 for the three train speeds. Most of the differences in the response due to this approximation occur for frequencies below 4 Hz for train speed 50 km/h; above 4 Hz the differences are small (less than 5 dB). For the higher train speeds 150 and 300 km/h there is a good agreement in the response above 10 Hz and 20 Hz respectively, which is where the highest responses generally occur (see Figures 3 and 4).

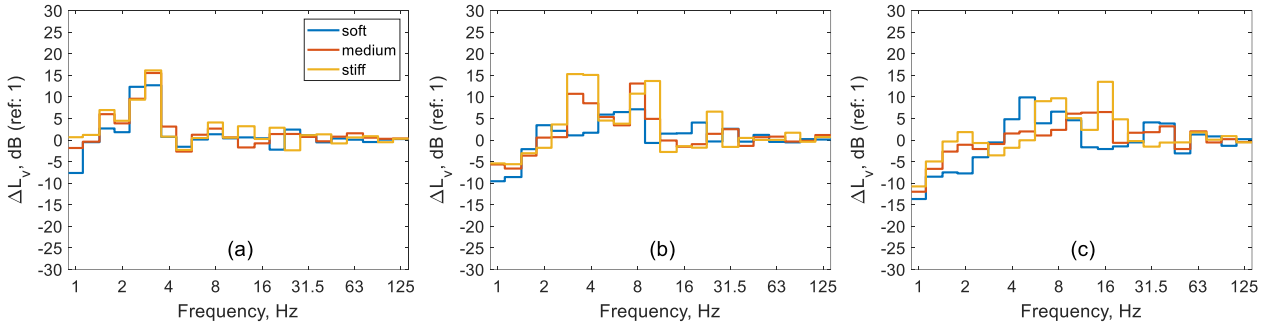

Figure 9: Free field vibration level difference ΔL_v between the incoherent (non-moving) load approximation and the coherent (non-moving) load reference case at 8 m from the track for the IC train running with (a) 50 km/h, (b) 150 km/h and (c) 300 km/h.

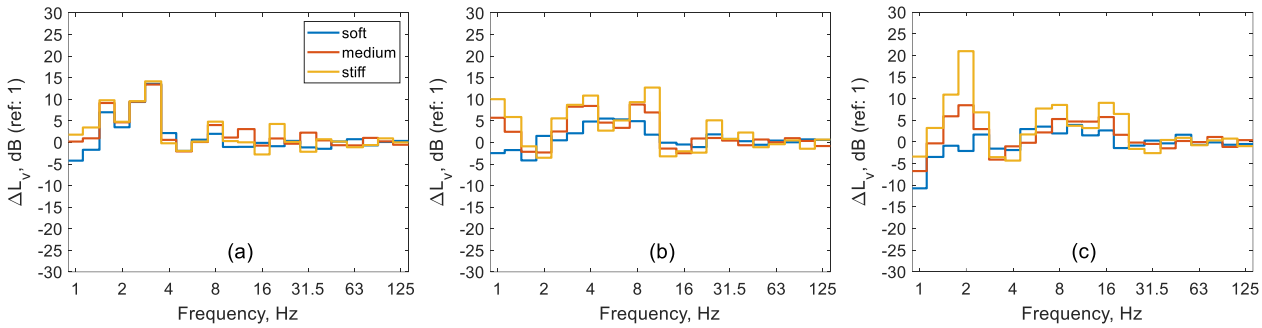

Figure 10: Free field vibration level difference ΔL_v between the incoherent (non-moving) load approximation and the coherent (non-moving) load reference case at 32 m from the track for the IC train running with (a) 50 km/h, (b) 150 km/h and (c) 300 km/h.

3.6. Overall effect of modelling assumptions

Of the three approximations discussed above, the moving axle loads have the largest influence whereas the assumption of independent axle loads mainly affects the response at low frequencies. The effect on the track compliance is negligible. The combined effect of all three approximations is shown in Figures 11 and 12 for the example speed of 150 km/h. The curves labelled 'reference' are the full predictions including all effects and those labelled 'approximation' include all three approximations. It is clear that, although there are significant differences in individual frequency bands, the overall spectrum shape is closely followed. The overall vibration level summed over all frequency bands is on average 2-3 dB higher for the models including all approximations than the complete models. This is consistent with results given in [9].

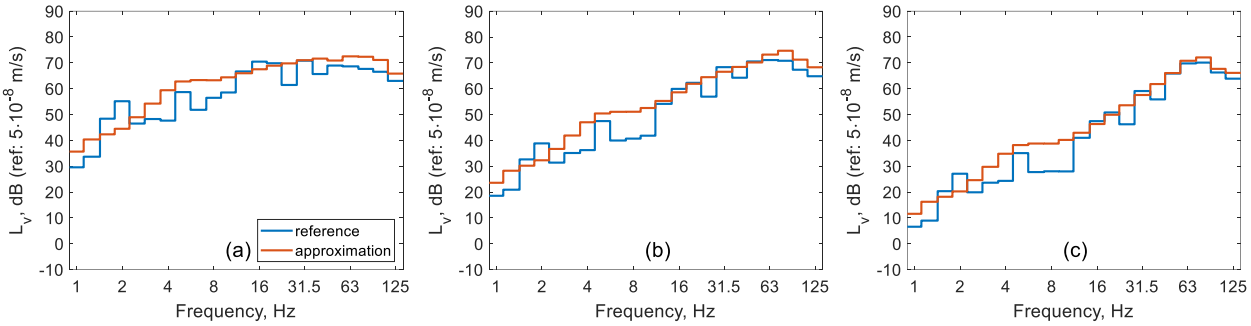

Figure 11: Effect of modelling assumptions on free field vibration level L_v at 8 m from the track for the IC train running at 150 km/h for the (a) soft soil, (b) medium soil and (c) stiff soil.

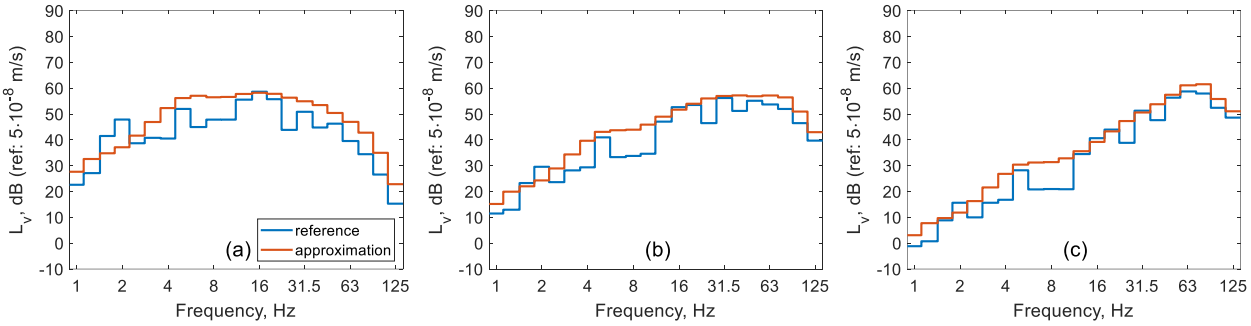

Figure 12: Effect of modelling assumptions on free field vibration level L_v at 32 m from the track for the IC train running at 150 km/h for the (a) soft soil, (b) medium soil and (c) stiff soil.

4. CONCLUSIONS

In the SILVARSTAR project a hybrid frequency-based prediction tool is developed that provides a flexible and efficient approach to predicting ground vibration from railways. This relies on a number of modelling assumptions that have been investigated here.

The track compliances can be calculated safely neglecting the influence of load speed. However, the Doppler shift leads to large differences in the response in individual frequency bands at higher speeds. Nevertheless, these differences mainly correspond to a redistribution of energy into different bands and the overall level is affected much less. Assuming that the dynamic axle loads can be treated as incoherent has a significant effect at low frequency but has negligible effect at the higher frequencies that are generally dominant in the spectrum.

Overall, although the proposed approach involves compromises to achieve efficient calculations, the differences introduced by these approximations are stronger in individual frequency bands and have much less effect on the overall vibration spectrum. The overall vibration levels are consistently 2-3 dB higher when including the various approximations.

5. ACKNOWLEDGEMENTS

The work presented in this paper has received funding from the Europe's Rail Joint Undertaking under the European Union's Horizon 2020 research and innovation programme (grant agreement no. 101015442). The contents of this publication only reflect the authors' views; the Joint Undertaking is not responsible for any use that may be made of the information contained in the paper.

6. REFERENCES

1. Thompson, D.J., Kouroussis, G., & Ntotsios, E. Modelling, simulation and evaluation of ground vibration caused by rail vehicles. *Vehicle System Dynamics*, **57**, 936–983 (2019).
2. https://silvarstar.eu/
3. Degrande, G., Lombaert, G., Ntotsios, E., Thompson, D., Nélain, B., Bouvet, P., Grabau, S., Blaul, J. & Nuber, A. State-of-the-art and concept of the vibration prediction tool. SILVARSTAR Deliverable D1.1, May 2021.
4. Quagliata, A., Ahearn, M., Boeker, E., Roof, C., Meister, L. & Singleton, H. Transit Noise and Vibration Impact Assessment Manual. FTA 0123, U.S. Department of Transportation, Federal Transit Administration, John A. Volpe National Transportation Systems Center, September 2018.
5. International Organization for Standardization. ISO 14837-1:2005 Mechanical vibration - Ground-borne noise and vibration arising from rail systems - Part 1: General guidance, 2005.
6. Villot, M., Guigou, C., Jean, P. & Picard, N. Definition of appropriate procedures to predict exposure in buildings and estimate annoyance, RIVAS project (SCP0-GA-2010-265754), Deliverable D1.6, June 2012.
7. Ntotsios, E., Thompson, D. & Hussein, M.F.M. A comparison of ground vibration due to ballasted and slab tracks. *Transportation Geotechnics*, **21**, 100256 (2019).
8. Lombaert, G., François, S. & Degrande, G. TRAFFIC Matlab toolbox for traffic induced vibrations. Report BWM-2012-10, Department of Civil Engineering, KU Leuven, November 2012. User's Guide Traffic 5.2.
9. Verbraken, H. Prediction of railway induced vibration by means of numerical, empirical, and hybrid methods. PhD thesis, Department of Civil Engineering, KU Leuven, 2013.
10. Nélain, B., Vincent, N. & Reynaud, E. Towards hybrid models for the prediction of railway induced vibration: numerical verification of two methodologies. In: G. Degrande, et al. (Eds) *Proceedings of 13th International Workshop on Railway Noise*. Ghent, Belgium, 16-20 September 2019, *Notes on Numerical Fluid Mechanics and Multidisciplinary Design*, **150**, 437-444 (2021).